International Information and Engineering Technology Association

Advancing the World of Information and Engineering

Energy-Efficient Design Optimization of Two-Bladed Agitators in Cylindrical Tanks

Sarra Youcefi[1*] , Abderrahim Mokhefi[2] , Mohamed Bouzit[3] , Abdelkader Youcefi[4]

[1] Department of Mechanical Engineering, University of Sciences and Technology of Oran, 1505 El Mnaouer, Oran 31000, Algeria

[2] Modeling and Experimentation Laboratory L2ME, Bechar University, B.P.417, Bechar 08000, Algeria

[3] Laboratory of Maritime Sciences and Engineering, University of Science and Technology of Oran, BP 1505 El-Mnaouer, Oran 31000, Algeria

[4] Laboratory of Aeronautics and Propulsion Systems, University of Science and Technology of Oran, BP 1505 El-Mnaouer, Oran 31000, Algeria

Corresponding Author Email: sarra.youcefi@univ-usto.dz

ABSTRACT

This study delves into the three-dimensional hydrodynamics of a flat-bottomed cylindrical tank equipped with a two-bladed impeller of various shapes, operating under laminar conditions. The focus is directed towards comprehending the flow patterns and power requirements necessary for mixing an incompressible Newtonian fluid using these two-blade agitators. Employing a novel design approach, the study introduces a unique configuration of the impeller, comprising two juxtaposed sub-two-blade sections, each mirroring the volume, diameter, and height of the standard impeller. The research examines the effects of the enlarged part's height and explores a range of Reynolds numbers from 10^{-1} to 10^2. A significant innovation of this investigation is the formulation of new agitator designs, specifically tailored to diminish power consumption while enhancing the mixing efficiency. The newly designed agitator shapes exhibit turbine-like characteristics, not only generating tangential velocities but also promoting increased axial velocities. This leads to the formation of secondary flows around the blade, a key factor in the improved mixing process. Results from the study demonstrate that this innovative agitator configuration markedly reduces energy consumption, thereby achieving enhanced power efficiency. These findings carry substantial implications for optimizing mixing processes in industrial applications, offering potential pathways for cost savings and operational efficiency improvements.

1. INTRODUCTION

Mechanical agitation plays a pivotal role in industries such as chemicals, pharmaceuticals, food, paint, and wastewater treatment. A critical challenge faced in these sectors involves reducing energy consumption and optimizing mixing time for efficient operations, a problem partially addressed in previous research [1, 2].

In industrial settings, stirred tanks of various shapes, equipped with simple and complex agitators, are commonplace. The design of agitator blades emerges as a crucial parameter in mixing systems, a subject extensively studied in numerous research laboratories globally. Ameur et al. [3] developed a novel blade design aimed at minimizing energy consumption while enhancing mixing quality, factors that directly influence the cost of mixing operations. Their research analyzed the effects of blade curvature, diameter, and number. The findings indicated that curved blades are more effective in reducing energy consumption compared to straight blades. Bouzit et al. [4] conducted a numerical simulation in a tank filled with a Newtonian fluid, stirred by a two-bladed agitator. This study confirmed that such geometries predominantly generate tangential flow, with the second agitator behaving akin to a turbine, generating higher axial and radial speeds. The influence of the agitator's position within the tank on axial velocity was also examined. Laidoudi [5] numerically simulated the flow in a tank stirred by a two-bladed agitator with holes of varying diameters. Results showed that blades with a hole diameter ratio of 0.133 enhance mixing speed and decrease the power number. Abid et al. [6] simulated the flow of viscous fluids in a vessel stirred by two blades of different heights, observing that agitator size significantly impacts flow structure. Foukrach et al. [7] compared the effects of a three-blade Rushton turbine shape on energy consumption and vortex size, revealing that turbines with converging triangular blades increase power consumption, while those with diverging triangular blades reduce vortex size. Devi and Kumar [8] analyzed flow characteristics in a stirred tank using a curved blade impeller, identified as the most efficient type. Luan et al. [9] employed a novel curved six-blade turbine to improve mixing time and energy consumption in a resolubilizing fluid, noting that mixing rate and efficiency are influenced by turbine eccentricity and clearance from the tank bottom. Youcefi et al.

[10] observed a significant reduction in energy consumption and vortex size in a slotted stirred tank with a Rushton turbine. Hassouni et al. [11] demonstrated that thermal effects enhance mixing quality in a four-bladed turbine-agitated tank, with no discernible influence of the Richardson number on the power number. Finally, Kamla et al. [12] conducted a comparative study of three modified anchor-type agitator geometries, aiming to improve fluid mixing in tanks and reduce energy consumption, especially in the lower part of the tank.

In the realm of agitation systems, the power number stands as a critical global parameter, intricately linked to the flow structures determined significantly by the agitation system design and fluid rheology. The pursuit of reducing energy consumption has captivated many researchers in this field. Youcefi and Youcefi [13] conducted measurements of the power number and mixing time in a tank stirred by a two-blade mobile in viscoelastic fluids, revealing a strong dependence of mixing time on fluid elasticity. Ameur and Bouzit [14] embarked on a numerical study to investigate energy consumption and velocity profiles in a flat-bottomed cylindrical tank agitated by a two-blade mobile, focusing on both Newtonian and non-Newtonian rheofluidifying fluids. They established a correlation for estimating energy consumption, taking into account variations in Reynolds number, fluid flow index, and blade dimensions. Yang et al. [15] demonstrated that, for equivalent power consumption, the velocity components in a stirred tank with RT-G are enhanced in comparison to those in RT. Basavarajappa et al. [16] observed the highest power number values with larger agitator sizes, noting a substantial decrease of nearly 70% in power number when the bottom clearance was reduced from 60 to 100 mm for the second turbine. Ge et al. [17] through simulation studies, found that alterations in blade shape significantly affect velocity distribution and energy consumption. Kato et al. [18, 19] correlated the energy consumption of various wide Maxblend type impellers using established expressions from the literature. Haitsuka et al. [20] investigated energy consumption and the volumetric mass transfer coefficient in tanks fitted with diverse impellers, concluding that larger impellers do not necessarily reduce aerated energy consumption. Lane and Koh [21] employed numerical methods to calculate the flow and power dissipation in a tank baffled by a Rushton turbine, contributing further to the understanding of energy dynamics in agitation systems.

In the field of agitation, researchers have increasingly focused on utilizing both numerical and experimental simulations to enhance hydrodynamic performance in tanks containing various types of fluids, including complex fluids, suspensions, and nanofluids. Youcefi [22] conducted an experimental investigation into the power number, mixing time, and velocity profiles for viscoelastic fluids in a cylindrical tank stirred by a two-blade mobile. His findings indicated a decrease in power number at a Reynolds number Re*=7. Bertrand [23], in his study on the agitation of Newtonian and non-Newtonian fluids using paddle, anchor, and barrier mobiles, applied both numerical and experimental techniques. Ameur [24, 25] explored the impact of blade inclination on the flow of non-Newtonian fluids in a stirred tank. The results demonstrated an increase in both the power number and vortex size with shear thinning and the angle of attack of the blades. Energy consumption was observed to increase significantly when the blade height ratio was adjusted from 0.1 to 0.95 and the blade diameter ratio from 0.2 to 0.8. Mokhefi et al. [26, 27] studied the thermal and hydrodynamic

effects of a non-isothermal laminar flow of an Al_2O_3-water nanofluid in both standard and wavy tanks equipped with an anchor. They concluded that optimal heat transfer was achieved with a high-volume fraction nanofluid and a low behavior index, and corrugated walls contributed to high thermal efficiency. Montante et al. [28] compared mixing times determined through Computational Fluid Dynamics (CFD) with experimental data obtained using a conductimetric method for rheofluidifying fluids. They also examined the influence of tracer injection position on mixing time. Wang et al. [29] presented findings on the energy required for suspension in a mechanically agitated tank, suggesting that solid suspensions could be enhanced by removing baffles. Pakzad et al. [30] utilized CFD data to study the effects of turbine power, fluid rheology, and turbine size on the mixing time of rheofluidifying fluids.

Upon conducting a thorough review of existing literature in the field of mixing, it becomes clear that the design of the agitator is crucial in optimizing mechanical agitation performance. Despite this, there is a notable gap in the literature regarding two-blade agitators, particularly in terms of enhancing hydrodynamic mixing processes and reducing energy consumption. These agitators are especially relevant in the context of highly viscous fluids, where energy efficiency is a significant concern, and axial movements are typically minimal. However, the introduction of some axial motion is necessary to disrupt stagnation at the bottom of the tanks. Addressing this gap, the current study aims to develop novel agitator configurations that not only enhance axial mobility but also preserve the predominance of tangential motion. This geometric approach to improving flow behavior and energy efficiency represents a novel area of exploration, absent in the existing body of research. This gap thus forms the primary motivation for this investigation, promising to contribute significantly to the field of mechanical agitation.

2. MIXING SYSTEM DESCRIPTION

Figure 1(a) illustrates the standard geometric configuration of the stirred system, comprising a flat-bottomed cylindrical tank with a diameter D and height H.

The mechanical stirring unit consists of a two-blade device composed of two vertical flat blades with a height h, diameter d, and thickness t sufficient to prevent any deformation during stirring. This impller rotates with a rotational speed N. To avoid scraping the tank's bottom, the agitator is positioned at a distance c and fixed to a central cylindrical shaft with a diameter da. The fluid used in this study is water at 25°C, exhibiting Newtonian properties, with a density of ρ=997 kg/m³ and a dynamic viscosity of μ=8.9×10⁻⁴ Pa·s.

Due to the significant importance of the mixing process, especially in the presence of highly viscous fluids, it has been recognized the necessity of contemplating the design of a new form for the two-blade agitator. This design aims to contribute to the enhancement of vessel bottom dynamics and the reduction of energy consumption. In this context, and in comparison, to turbine operations, it has been expected that the design should consist of two parts, one being wide and the other narrow. Nevertheless, a computational analysis is required to explicitly evaluate the effectiveness of this design in both dynamic and energy aspects.

The standard two-blade impeller has been modified to create a pseudo-two-blade impeller composed of two

juxtaposed agitating parts. The shape of each of these parts resembled a two-blades but with different diameters and heights. The first lower part, has the largest diameter which equals to the diameter of the standard impeller d. The design aimed to create two-blade according to the proposed configuration, with the heights h_m of the first part of the two-blade being varied. The performance of the resulting mixing system based on these different heights will be analyzed in the present investigation, see Figure 1(b). This figure shows a stirred tank equipped with the modified two-blade stirrer presenting several designs with different height ratios h_m/h ranging from 0 to 1. All the geometric parameters of the mixing system are shown in Table 1.

(a) Standrad impeller (b) Modified impeller
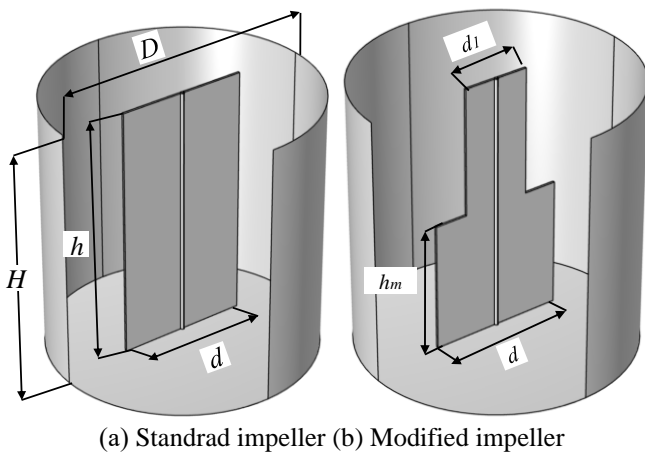
Figure 1. Geometry and dimensions of the mixing system

Table 1. Geometric parameters of the stirred system

D [mm]	H/D	d/D	h/D	c/D	t/D	d_a/D	d_1/D
300	1	0.5	0.966	0.033	0.008	0.016	0.25

The proposal of a new agitator configuration and the assessment of its impact on energy and hydrodynamic behavior are of important significance. For instance, a new configuration aimed at reducing the amount of material used in the agitator's design naturally leads to a decrease in power consumption due to the reduced volume of swept fluid. To avoid any energy consumption dependency, it has been deemed necessary to perform the present calculations by proposing a two-blade design with a volume equal to that of the standard two-blade agitator. Hence, this new design is created with increased thickness compared to the standard version, thus compensating for the reduced volume in the upper part of the new two-blade agitator. If Vo_s and Vo_m represent respectively the volumes of the standard and modified two-blade, and t_s and t_m their thicknesses, then:

$$Vo_s = Vo_m \tag{1}$$

Based on Eq. (1) and by substituting the expressions for the volumes Vo_s and Vo_m as a function of the agitator geometric parameters namely d, d_1, h, h_m and t_s, the thickness (t_m) of the new two-blade configuration can be calculated using the following expression:

$$t_m = \frac{dht_s}{dh_m + d_1(h - h_m)} \tag{2}$$

3. MATHEMATICAL EQUATIONS

A theoretical analysis of the hydrodynamic and energy performance of agitated systems, particularly the current agitation system, relies on a thorough understanding of fluid flow velocity (u, v, w) and pressure p at every point. In experimental analysis, these two parameters are determined using measuring instruments. However, in theoretical analysis, they are established by solving a set of differential mathematical equations known as the Navier-Stokes equations. The flow inside the agitated tank equipped with the new two-blade impeller design is hence governed by the fundamental equations of Computational Fluid Dynamics of Navier-Stokes, including mass and momentum equations. Adopting Cartesian coordinates and laminar stationary regime, the governing equations are given as follow:

Mass equation

$$\frac{\partial u}{\partial x} + \frac{\partial v}{\partial y} + \frac{\partial w}{\partial z} = 0 \tag{3}$$

Momentum equations

$$\rho\left(u\frac{\partial u}{\partial x} + v\frac{\partial u}{\partial y} + w\frac{\partial u}{\partial z}\right) = -\frac{\partial p}{\partial x} + \mu\left(\frac{\partial^2 u}{\partial x^2} + \frac{\partial^2 u}{\partial y^2} + \frac{\partial^2 u}{\partial z^2}\right) \tag{4}$$

$$\rho\left(u\frac{\partial v}{\partial x} + v\frac{\partial v}{\partial y} + w\frac{\partial v}{\partial z}\right) = -\frac{\partial p}{\partial y} + \mu\left(\frac{\partial^2 v}{\partial x^2} + \frac{\partial^2 v}{\partial y^2} + \frac{\partial^2 v}{\partial z^2}\right) \tag{5}$$

$$\rho\left(u\frac{\partial w}{\partial x} + v\frac{\partial w}{\partial y} + w\frac{\partial w}{\partial z}\right) = -\frac{\partial p}{\partial z} + \mu\left(\frac{\partial^2 w}{\partial x^2} + \frac{\partial^2 w}{\partial y^2} + \frac{\partial^2 w}{\partial z^2}\right) - \rho g \tag{6}$$

In the present study, the rotational speed of the impeller is commanded by the Reynolds number which is calculated for the modified impeller using the characteristic dimension d (diameter of the largest part two-blade):

$$\text{Re} = \frac{\rho N d^2}{\mu} \tag{7}$$

The power number Np is a dimensionless parameter used in fluid mechanics and chemical engineering to characterize the power consumption of an agitator or impeller in a mixing process. It represents the ratio of the power input to the fluid by the agitator to the power input required for ideal, uniform mixing. The power number is essential for understanding the efficiency and effectiveness of mixing equipment and is often used to compare different agitator designs and their performance in various mixing applications. In the case of the current modified two-blade agitator, the power number using the following formula:

$$Np = \frac{P}{\rho N^3 D^5} \tag{8}$$

where, P denotes the power consumed by the stirred system. It can be calculated using the viscous dissipation function.

$$P = \mu \iiint\limits_{\text{Vessel volume}} Q_v \mathrm{d}x \, \mathrm{d}y \, \mathrm{d}z \qquad (9)$$

where, Q_v presents the viscous dissipation function which is calculated based on the fluid flow velocities (u, v, w) within the agitated vessel, obtained from Eqs. (3)-(6), using the following formula:

$$Q_v = 2\left(\frac{\partial u}{\partial x}\right)^2 + 2\left(\frac{\partial v}{\partial y}\right)^2 + 2\left(\frac{\partial w}{\partial z}\right)^2 + \left(\frac{\partial u}{\partial y} + \frac{\partial v}{\partial x}\right)^2 + \left(\frac{\partial u}{\partial z} + \frac{\partial w}{\partial x}\right)^2 + \left(\frac{\partial v}{\partial z} + \frac{\partial w}{\partial y}\right)^2 \qquad (10)$$

The tangential, radial, and axial velocities play an important role in the study of fluid agitation in a mixing system. They allow to characterize the fluid movements induced by the agitator, which is essential for understanding the performance and efficiency of the mixing process. The tangential and the radial velocities are calculated according to the Cartesian velocities u and v as follow:

$$V_\theta = \frac{-uy + vx}{\sqrt{x^2 + y^2}}, \quad Vr = \frac{ux + vy}{\sqrt{x^2 + y^2}} \qquad (11)$$

It should be noted here that the axial velocity is equal to w in the Cartesian referential. On the other hand, it is worth noting that the results will be presented with dimensionless quantities allowing to normalize physical quantities and generalize the study. Hence, certain dimensionless quantities, namely the tangential, radial, and axial velocities are defined as follows:

$$V_\theta^* = \frac{V_\theta}{\pi ND}, \quad V_r^* = \frac{V_r}{\pi ND}, \quad W^* = \frac{w}{\pi ND} \qquad (12)$$

4. NUMERICAL METHOD

4.1 Numerical detail

The finite element method has been employed to solve the system of equations with boundary conditions. It is important to mention that these governing equations are presented in this paper within a fixed frame of reference. However, when dealing with flows induced by rotating machines, it is more convenient to solve the governing system in a moving reference frame. This approach simplifies the consideration of rotation, particularly when the machines do not have a cylindrical shape. As a result, all the equations have been reformulated in a moving reference frame.

In the present study, the flow has been simulated using MRF (Multiple Reference Frame) technique. With the MRF technique, the computational domain is divided into two volumes: a rotating inner cylindrical volume containing the two-bade and a stationary outer volume containing the rest of the tank.

Due to the complexity of the geometry of the agitated system, which includes both a cylinder and parallelepipeds, the mesh chosen has a generally tetrahedral shape. Indeed, this form of meshing in such geometries gives a significant result,

especially near complex regions. Therefore, the adopted mesh has a non-structural tetrahedral shape and is refined near the walls of the two-blade and the tank, see Figure 2. The convergence of the results was achieved when the residual reached a level close to 10^{-6}, and the field values remained almost unchanged over the last 4000 iterations.
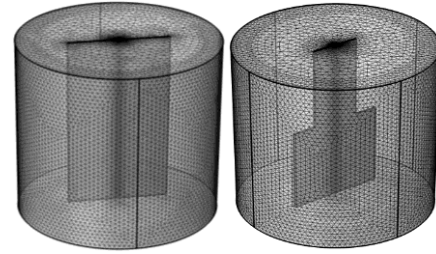
Figure 2. Mesh of the computational domain

4.2 Mesh check

In order to ensure the agreement of the present results and to approach those of the literature, several meshes have been tested.

Table 2 shows the number of elements used in the simulation and the evolution of the values of the power number Np, which is characteristic of mechanical agitation. After the analysis of the variation of the power number values according to three meshes (M1-M3), a mesh containing 814796 tetrahedral elements (mesh M2) has been opted for, beyond which the values of the power number remain practically unchanged, as shown in Table 2.

Table 2. Variation of power number as function of elements number

Mesh	M1	M2	M3
Elements	258365	814796	1181235
Power number	17.932	18.8210	18.8260

4.3 Code validation

Prior to conducting any numerical study, it is essential to validate the results using the experimental data available in the literature. This validation is performed under the same geometrical parameters and flow conditions as those used in the experimental works of Youcefi [22] and Ameur [24]. In Figure 3, the tangential velocity variation with respect to the vessel radius is depicted for Re=4. Remarkably, the numerical results demonstrate excellent agreement with the experimental data, reaffirming the accuracy and reliability of the computational model employed in this study. This congruence in the results further validates the predictive capabilities of our numerical approach and establishes confidence in its ability to capture the intricacies of the fluid dynamics within the system.

The close correspondence between the numerical and experimental findings underlines the significance of the simulation and lends credibility to the obtained results.

Table 3 presents the variation of the power number as a function of the Reynolds number for the current simulation, along with the references from Bertrand [23] and the correlation proposed by Ameur and Bouzit [14]. The results demonstrate a good level of agreement among the datasets. It is worth noting that the percentage of deviation between the numerical results and the other references for all cases of Reynolds number does not exceed 7.5%, which indicates an

excellent level of consistency and accuracy in our numerical predictions.
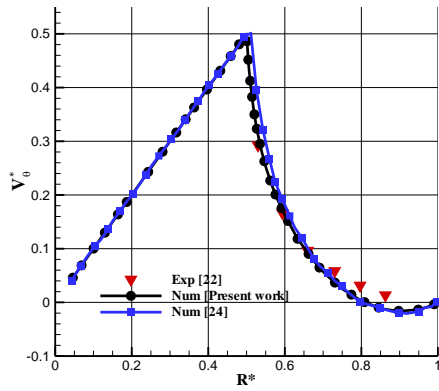
Figure 3. Tangential velocities along of the agitator plane and its extension to the vessel wall

Table 3. Comparison between power number for various values of Reynolds number

Reynolds Number	Experimental [23]	Correlation [14]	Present Work	Deviation
Re=10^{-1}	1751	1411.18	1818.67	3.86 %
Re=10^{0}	175.8	142.83	181.94	3.49 %
Re=10^{1}	20.08	14.45	18.65	7.12 %

5. RESULTS AND DISCUSSIONS

The hydrodynamic results of the new two-blades configuration shown in Figure 4 in the agitated tank have been analyzed in different planes and lines, as shown respectively in Figures 5 and 6. The influence of the parameters, namely the Reynolds number and the height of the enlarged part of the two-blades, on the hydrodynamic and energetic behavior in the agitated tank has been highlighted. The results are presented in the form of axial and radial tangential velocity contours, streamlines, and power number curves. For a purely laminar regime, a Reynolds number range between 0.1 and 100 has been adopted in this study. Moreover, following the design conditions, the shape ratio, defined as the height of the enlarged part of the two-blades relative to the height of the standard one, has been varied between 0 and 1.
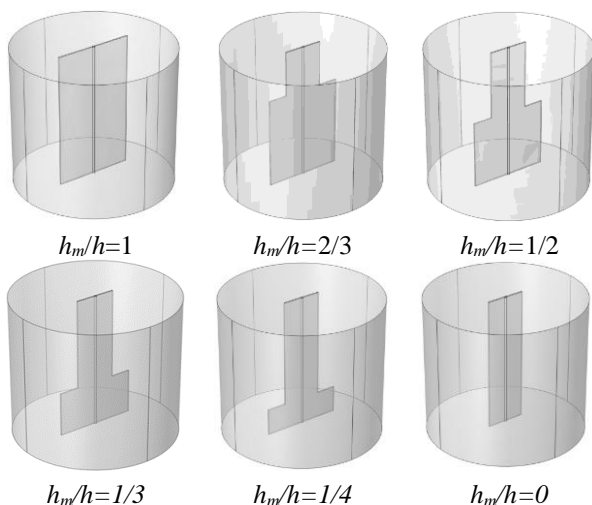
Figure 4. Different geometries of the suggested two-blades
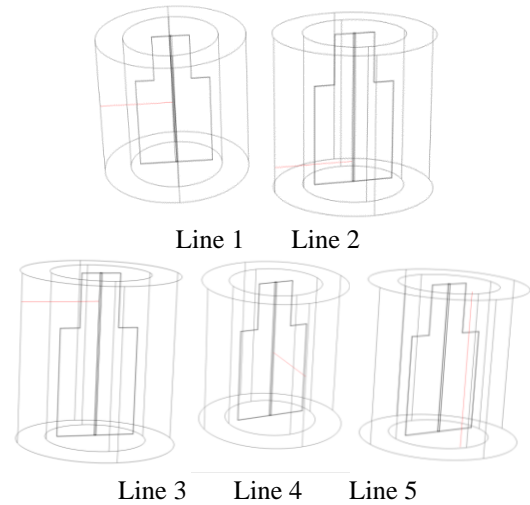
Figure 5. Different measurement lines adopted in the present analyze
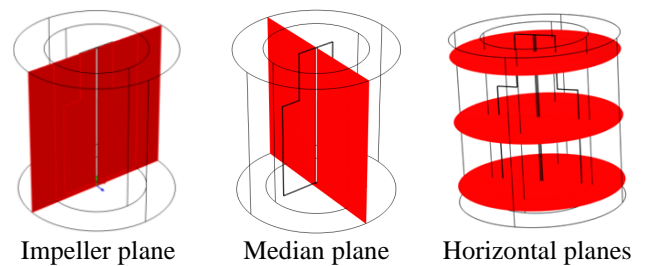
Figure 6. Different measurement planes adopted in the present analyze

5.1 Hydrodynamic behavior

In this subsection, we focus on analyzing the hydrodynamic behavior inside the agitated tank, taking into account the influence of the Reynolds number, which reflects in fact the rotational speed of the two-blade, as well as the height of its enlarged part of this impeller. The objective is to identify the different behaviors of the three velocity components namely tangential, radial and axial velocities, which are important for assessing the mixing quality. We aim to gain a better understanding of how these parameters affect the fluid flow in the tank and its ability to achieve efficient mixing. It is important to remember that the variation in height of the enlarged part of the two-blade is accompanied by the conservation of its total volume, and therefore, the same volume of fluid swept.

5.1.1 Global hydrodynamic behavior

For a more in-depth understanding, the global velocity contours and streamlines are presented in different planes, as shown in Figure 6.

Figure 7 illustrates the distribution of the velocity magnitude and the streamlines' behavior at the agitator plane, extending towards the tank wall for different heights of the enlarged part of the two-bale under two Reynolds number values: *Re*=10 and *Re*=30.

With varying the targeted height from h_m/h=1 to 0, regardless of the Reynolds number, a noticeable decrease in the overall kinetic intensity is observed in this plane as the height of the widened part decreases (where the largest height corresponds to the standard configuration).
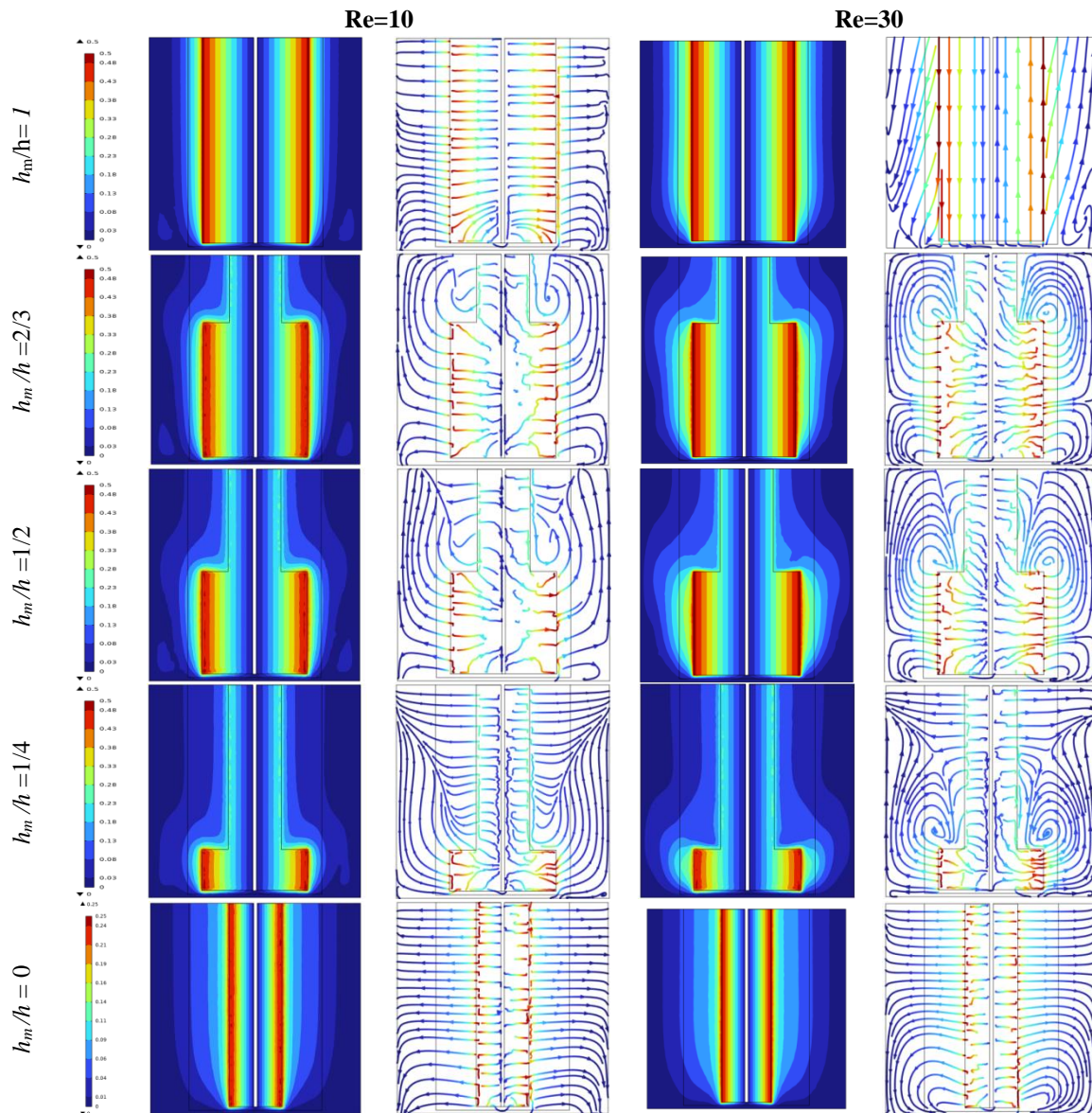
Figure 7. Velocity contours and streamlines in the plane of the agitator for two Reynolds number

However, it's worth noting that the maximum velocity remains constant and is equal to $d/D=0.5$ (dimensionless) except for the configuration with a height of 0, where this maximum velocity decreases to $d/D=0.25$. This decrease is attributed to the reduced overall diameter in this particular configuration. Furthermore, as the Reynolds number increases, the kinetic intensity becomes more pronounced, leading to higher velocities and stronger mixing effects.

As for the streamlines pattern, a transition from the standard configuration of the two-blade ($h_m/h=1$) to the modified configurations except for the case where $h_m/h=0$ reveals two coaxial symmetric vortices appearing in the upper part of the tank, particularly at high Reynolds numbers ($Re=30$). Additionally, in the case of the new configuration, two distinct vortices are developed near the tank bottom. The appearance of these vortices enhances the fluid circulation, leading to improved mixing efficiency and uniformity throughout the tank.

Moreover, in applications involving suspended particles, the bottom vortices permit in maintaining suspension, contributing hence to the overall effectiveness of the agitation process and preventing sedimentation

Regarding the modified configuration corresponding to

$h_m/h=0$, no additional advantages have been observed compared to the standard configuration. This specific setup essentially utilizes a standard two-blade, albeit with a reduced diameter and an increased thickness. In this particular case, the modifications made to the two-baled seem to have minimal impact on the hydrodynamic behavior inside the tank, as it retains the characteristics of a standard two-blade. Thus, it does not exhibit any significant improvement or alteration in the mixing performance, unlike the other modified configurations explored in the study.

Figure 8 illustrates the velocity magnitude contours and streamlines at the median plane of the tank for various heights of the two-blade studied at two Reynolds numbers, $Re=10$ and $Re=30$. Notably, the well-mixed zone in this plane diminishes in size as the height h_m decreases, with the exception of the last configuration. Interestingly, this zone aligns with the overall diameter of the agitator in the new shape, regardless of the Reynolds number. Regarding the streamline patterns, the two-blade modification leads to the emergence of four coaxial vortices, two in the upper and two in the lower part contrasting the two standard geometries ($h_m/h=0$ and 1) where the flow mainly remained tangential. These four vortices efficiently compensate for the kinetic deficit by introducing additional

zones of disturbance. These zones ultimately improve the mixing quality. Furthermore, as the Reynolds numbers increase, these vortices become more pronounced, significantly intensifying the flow. The observed formation of these vortices indicates a complex flow behavior resulting from the modified two-blade configurations, contributing to a more efficient and effective mixing process.

Figure 9 presents the distribution of iso-velocity values and streamline patterns at three horizontal planes within the studied agitation system, as indicated in Figure 6, for different two-blade designs, including the two standard shapes, at the previously selected Reynolds numbers. Starting with the two standard configurations (h_m/h=0 and 1), it is evident that the hydrodynamic behavior in all three measurement planes is almost identical. This similarity allows for a two-dimensional study, providing a comprehensive understanding of the standard two-blade operation away from the tank bottom.

Furthermore, two circular vortices, aligned with the direction of rotation and confined between the two-blade edges and the tank wall, are formed. However, these vortices gradually diminish and disappear with increasing rotational speed of the two-blade (Reynolds number). Upon modifying the two-blade configuration, the overall velocity decreases in the upper part of the tank but remains significant in the enlarged part of the modified two-blade. Particularly at Re=10, the vortices in this region are more pronounced but decrease as the Reynolds number increases.

Importantly, these two vortices in these planes exhibit regions of low circulation, often referred to as dead zones, which are effectively eliminated as the impeller rotational speed increases. The elimination of these dead zones with increasing agitator speed indicates a promising improvement in the mixing efficiency and minimizes areas of stagnant flow, leading to more effective mixing performance within the tank.
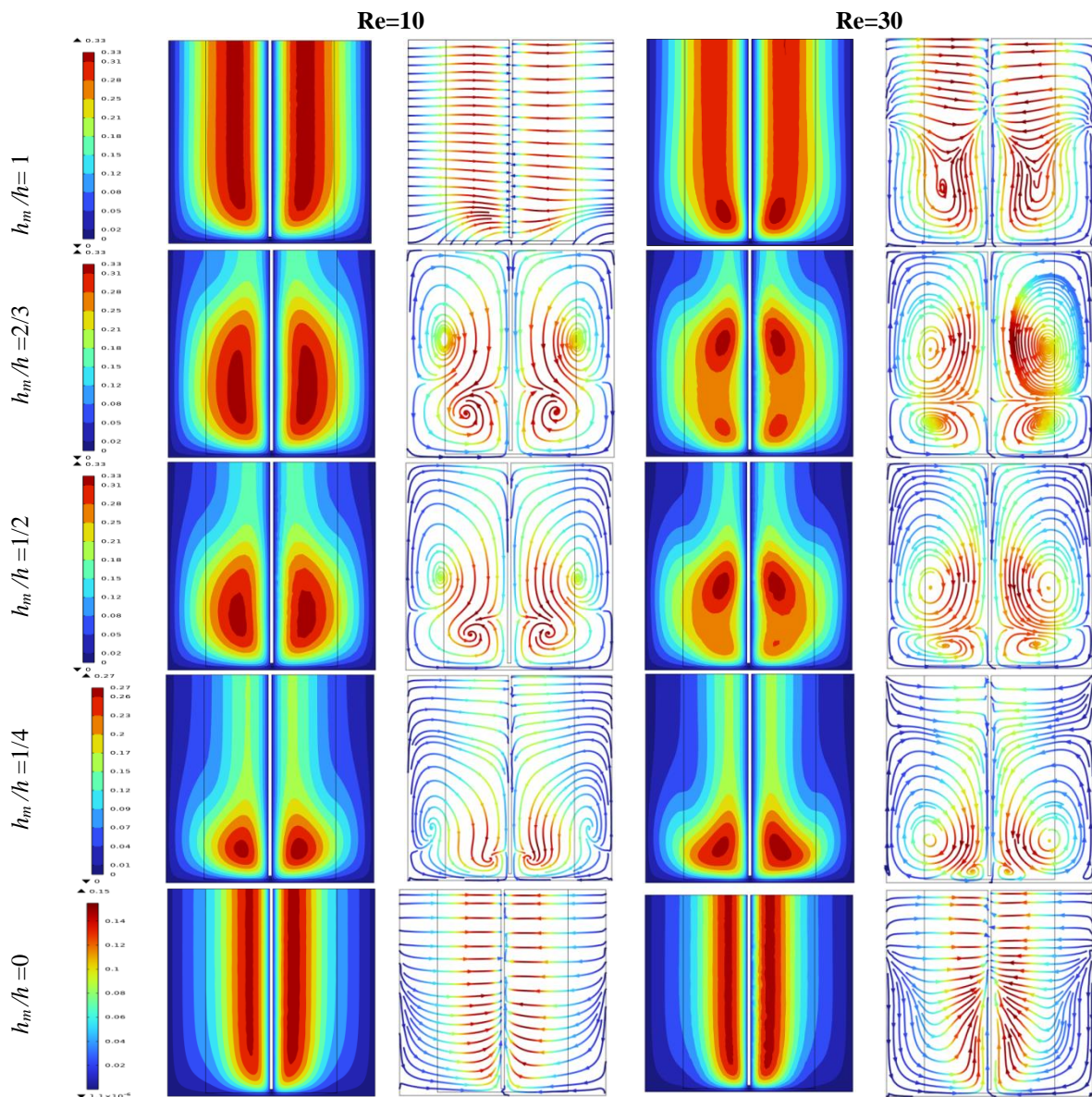
Figure 8. Velocity contours and streamlines on the median plan for two Reynolds number
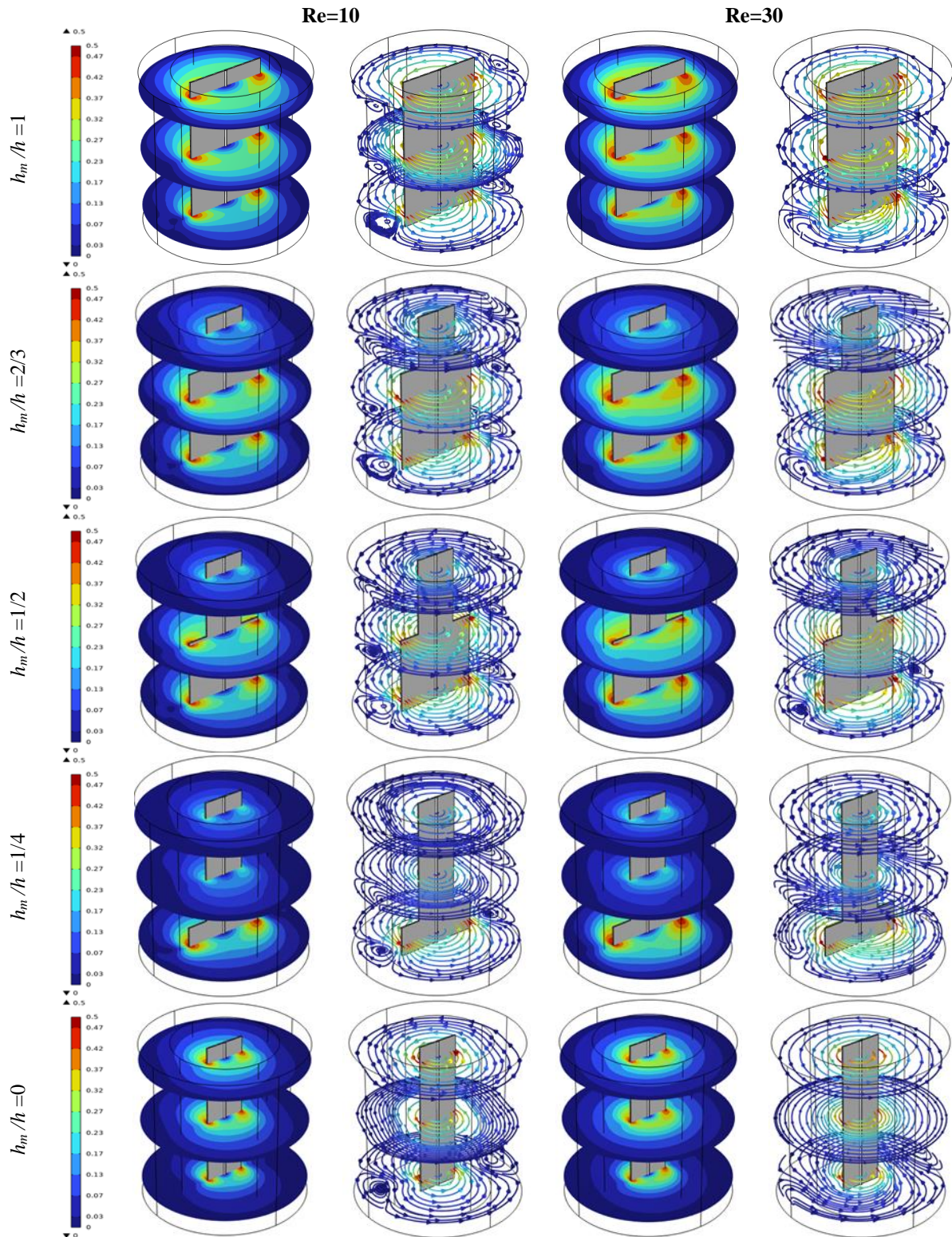
Figure 9. Velocity contours and streamlines on the horizontal planes for two different Reynolds numbers

Figure 10 presents the three-dimensional representation of the streamline patterns in the agitation system for the different two-blade designs, including the standard configurations, at two Reynolds numbers. This figure provides a comprehensive understanding of the fluid trajectory within the system. The projection of these trajectories onto the various planes coincide with the patterns previously discussed Notably, in the two standard two-blade configurations, the flow pattern remains entirely tangential due to the dominant parallelism of the streamlines with the horizontal planes. However, upon introducing the targeted modifications in the present study, this parallelism is disrupted, leading to an axial inclination of the streamlines.

This observation serves as an explanation for the formation of the previously discussed vortices, which primarily represent the vertical component of the fluid velocity. Therefore, a comprehensive analysis of the behavior of the three components of the velocity vector including tangential, radial and axial components is essential to better understand the hydrodynamics of our new impeller.
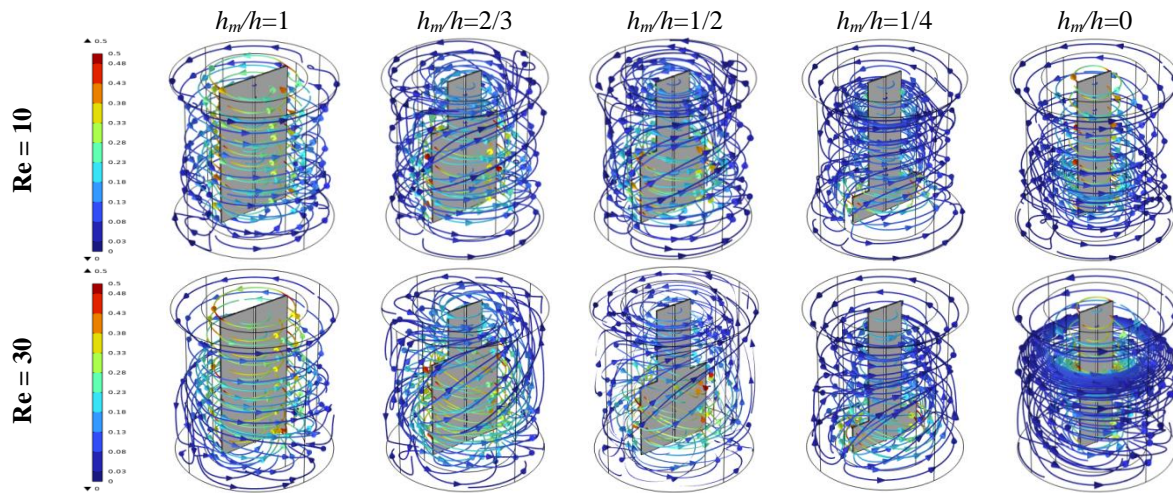
Figure 10. Tree-dimensional streamlines for different configurations of the two-blade

5.1.2 Specific hydrodynamic behavior

In this subsection, a more detailed analysis of the hydrodynamic behavior in the agitated tank equipped with the new two-blade configuration is presented. The analysis focuses on highlighting the behavior of the three velocity components during the modification of the agitator's geometry. The tangential, radial, and axial velocities are hence presented along the lines mentioned in Figure 5.

Figures 11 to 13 respectively depict the distribution of tangential, radial, and axial velocities along the five lines presented in Figure 5 for different heights h_m at Re=10.

Regarding the tangential velocity (Figure 11), along the various lines passing through the agitator plane and extending towards the tank walls (lines 1 to 4), a reduction is observed in the upper part of the new two-blade due to the decreased diameter in the new configuration (line 3). However, along the lines passing through the middle and bottom of this plane, the velocity remains quite similar to the standard cases, except for geometries with smaller h_m heights, where a reduction becomes evident (lines 1 and 2). Along the line passing through the median plane (line 4) and the vertical line (line 5), a distinct reduction in tangential velocity is noted with decreasing h_m height, even for the standard geometry with h_m/h=0. This reduction is attributed to the overall decrease in tangential kinetic energy, where the maximum velocities are found in the well-mixed zones. It is noteworthy that the tangential velocity along the vertical line strictly increases from the bottom of the tank to the free surface, creating a hydrodynamic boundary layer in the case of standard agitators (h_m/h = 0 and 1). However, for the modified configuration, the velocity profile exhibits a maximum, indicating the presence of well-mixed zones at specific locations between the tank bottom and the free surface. It should be noted that despite the decrease in tangential velocity, it still remains predominant. In other words, this does not represent a total loss.

Comparing with the tangential flow, the radial flow is relatively less. Along the lines passing through the agitator plane (lines 1 to 3) and the segments passing through the two-blade blades, the radial velocity initially remains negligible and then begins to manifest between the blade edges and the tank wall, displaying varying behavior for different impeller designs. The radial velocity's behavior indicates flow directed either towards the shaft or the tank wall, depending on the intensity of the tangential and axial velocity fields generated by the two-blade's hydrodynamics.

In the median plane line (line 4), a predominant inward flow towards the two-blade's shaft is observed, particularly for configurations with an intermediate height of h_m/h=1/3. This flow pattern arises due to the interference of various flows created by different parts of the new two-blade design. Notably, for configurations with h_m/h=2/3, the flow tends to direct towards the tank wall, driven by the predominant influence of the flow generated by the enlarged part of the impeller, especially at this specific Reynolds number (Re=10). The radial velocity along the vertical direction (line 5) exhibits variable behavior and becomes more significant for configurations that are intermediate between the two standard two-blades. Despite the considerable reduction in tangential flow resulting from the implementation of the new two-blade design, the emergence of vertical stream, as observed in the streamline figures, provides an insightful explanation for this phenomenon. Specifically, the curves presented in Figure 13 shed further interpretation on this behavior by examining the third velocity component, namely the axial velocity. This component exhibits a significant increase at various locations within the agitated tank when the new two-blade design is utilized (lines 1 to 5). Remarkably, in standard configurations (hm/h=0), as also examined by Youcefi [22] and Bouzit et al. [4], the axial velocity is practically negligible. However, with the introduction of the new two-blade design, the axial stream becomes a prominent feature of the flow. The effectiveness of the design in enhancing axial streams varies depending on the targeted regions within the tank. For instance, configurations with h_m/h=1/2 and 1/3 prove more effective in eliminating stagnation zones near the tank bottom (line 4). These findings elucidate the role of the axial velocity component in compensating for the reduced tangential flow caused by the new two-blade design. It is important to highlight that, based on the results and the assessment of axial velocity values, the modification technique aimed at increasing axial velocity seems to offer more advantages compared to the one employed by Bouzit et al. [4]. In their study, they made a radical change by transitioning from a two-blade agitator to a radial turbine, which led to a systematic loss of tangential flow, compensated by axial and radial flows. In contrast, our technique offers the advantage of preserving the tangential flow while introducing sufficient axial mobility to activate the lower zone.

The optimized designs with enhanced axial streams offer valuable insights for industries seeking to enhance mixing efficiency and reduce stagnant regions in their processes.
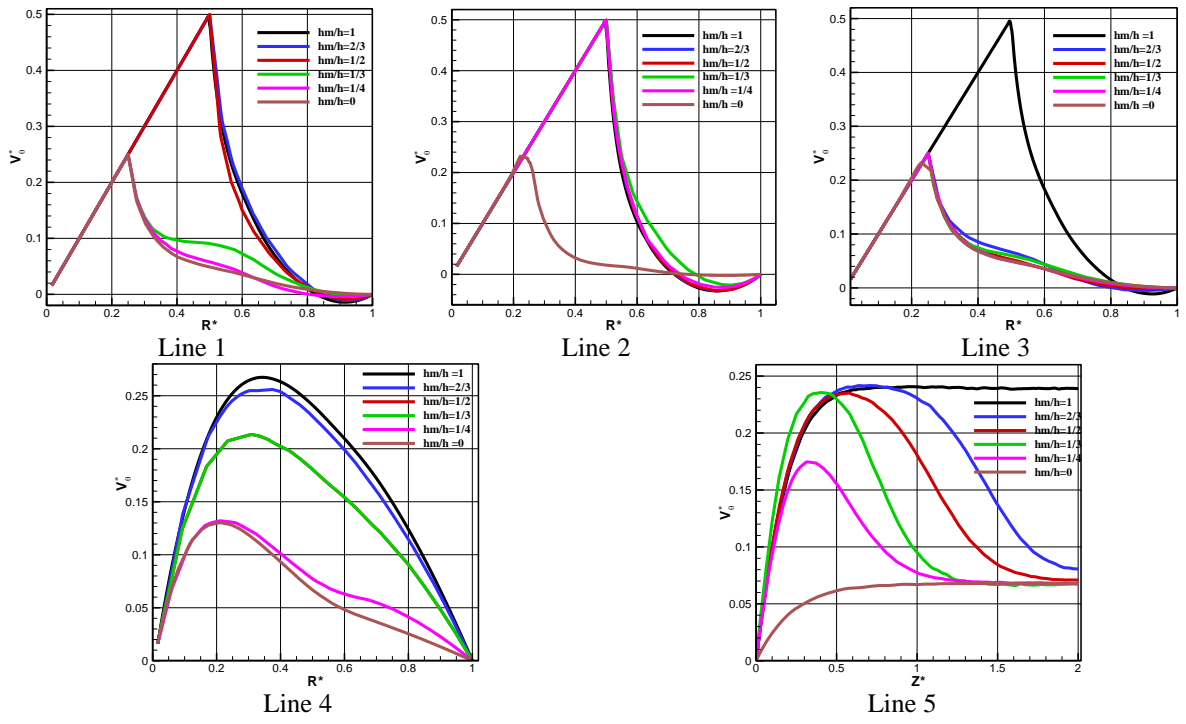
Figure 11. Tangential velocity for different geometries at different positions
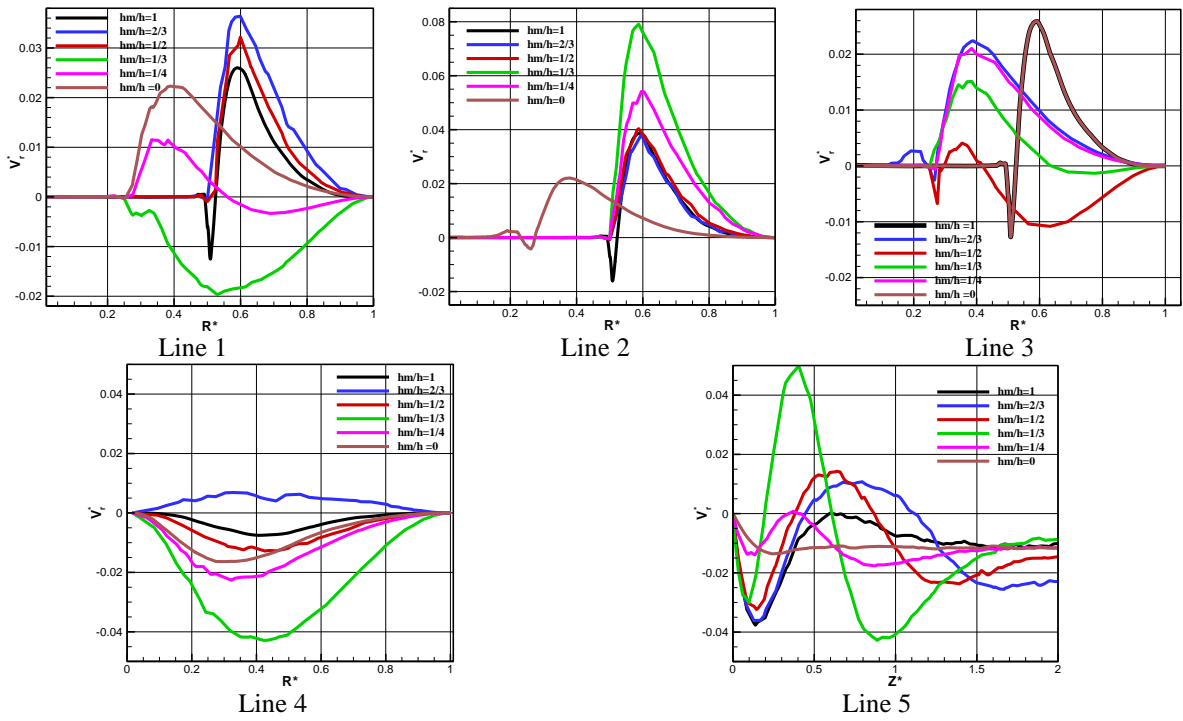
Figure 12. Radial velocity for different geometries at different positions
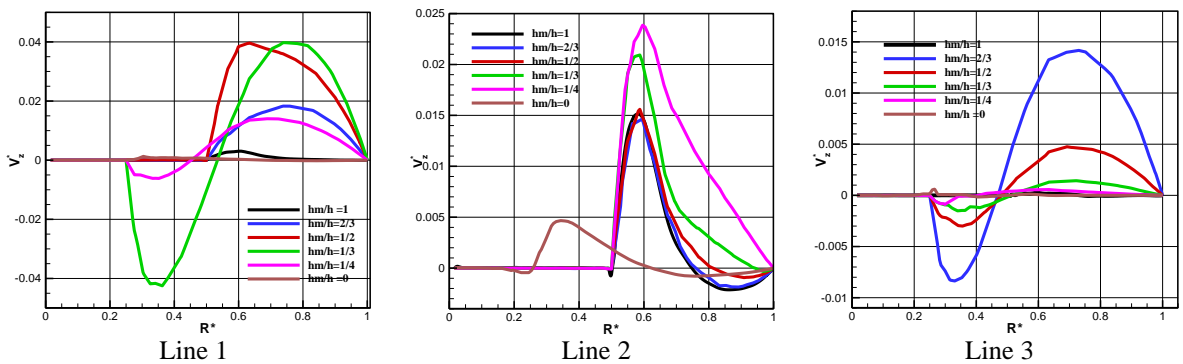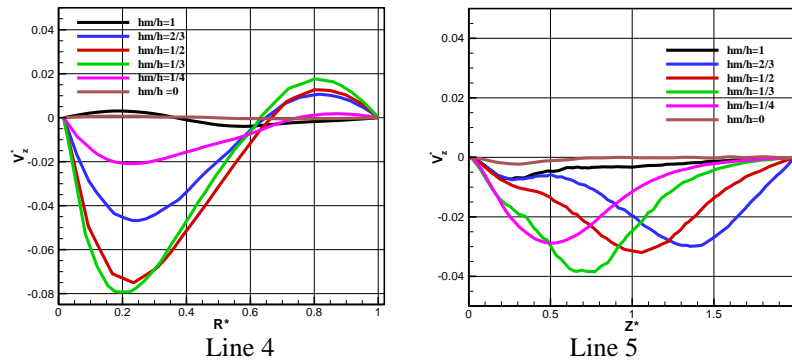
Figure 13. Axial velocity for different geometries at different positions

5.2 Power consumption

Agitation power, also known as mixing power, is an essential measure of the energy required to stir or mix a liquid in an agitated tank. It represents the amount of mechanical energy provided by the agitator to overcome shear forces and flow resistance of the fluid. The agitation power depends on several factors, such as the agitator's rotational speed, the type of agitator, the diameter and height of the agitator, the fluid's density and viscosity, the Reynolds number, and the tank's geometry. A lower power consumption is a sought-after advantage in the design of an agitator. A design that allows for the reduction of agitation power is beneficial in several ways. Therefore, it is essential to assess the power consumption rate of our agitation system with the new two-blade design featuring two expanded and narrowed parts in order to optimize the operating conditions. The power number is thus an indicator of consumed power.

Figure 14 depicts the power number of agitation as a function of the Reynolds number for different two-blade configurations, including the two standard geometries.
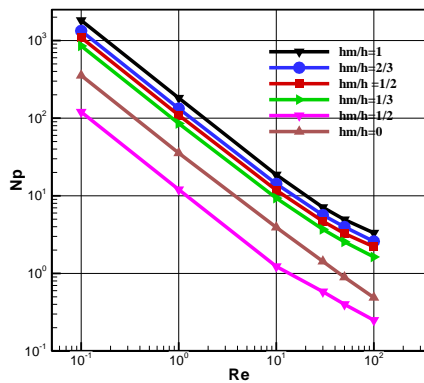
Figure 14. Power number versus Re for different geometries

The power number demonstrates a distinct decreasing trend as the Reynolds number increases, and it significantly diminishes with the implementation of the new design, especially for decreasing h_m values. This aspect represents a significant advantage of our research, as it indicates that we have achieved a more efficient and optimal energy consumption while simultaneously recovering the deficit in tangential movement. Importantly, this achievement has been accomplished while maintaining the same volume as the standard two-blade configurations, underscoring the important role of hydrodynamic modifications in reducing the power number.

In the case of the standard two-blade configuration with h_m/h=0, it is noteworthy that its power consumption is lower than that of the primary standard agitator but higher than the agitator with h_m/h=1/2. This discrepancy can be attributed to the variations in hydrodynamic behavior between the configurations, despite the volume being conserved.

Indeed, numerical data in tables can provide a more detailed view and allow us to identify the percentage of improvement in energy consumption compared to the primary standard case. Table 4 presents the power numbers and their corresponding percentage of improvement relative to the standard two-blade for various configurations and Reynolds numbers. At Re=10, a remarkable percentage improvement of 93.40% was achieved with a configuration having h_m/h=1/4. This specific design offers the most energy-efficient performance regardless of the Reynolds number. Additionally, the second standard geometry shows a substantial improvement percentage of 78.95% compared to the primary standard and ranks as the second-best geometry in terms of energy consumption.

Table 4. Power number for various modified height and Reynolds number

Np	$h_m/h = 1$	$h_m/h = 2/3$	$h_m/h = 1/2$
Re=10	18.65	14.26	11.81
%Np	--	23.53%	36.67%
Re=100	3.325	2.585	2.204
%Np	--	22.25%	33.71%
Np	$h_m/h = 1/3$	$h_m/h = 1/4$	$h_m/h = 0$
Re=10	9.338	1.230	3.924
%Np	49.93%	93.40%	78.95%
Re=100	1.630	0.250	0.489
%Np	50.97%	92.48%	85.29%

This knowledge can greatly benefit industrial applications seeking to enhance their energy efficiency and reduce operational costs.

It's worth noting that the approach taken in the current two-blade design yields better energy savings compared to the hole technique applied to two-blades as presented by Laidoudi [5], owing to several determinative factors. Furthermore, our technique, which combines axial mobility and tangential predominance, allows to minimize power consumption while sweeping the same volume of fluid without altering the blade's construction material. Consequently, the fluid's hydrodynamics is the only driver of this significant reduction. In contrast, in the hole technique, the analysis reveals an overall decrease primarily attributable to the reduction in the blade's construction material, which is not as straightforward.

6. CONCLUSIONS

In this study, an in-depth investigation on the effect of a new modified design of the two-blade impeller has been conducted. By forming two juxtaposed sub-blades, one enlarged and the other narrowed, our aim was to improve the hydrodynamic behavior and optimize power consumption in the agitated tank. The present findings revealed several important conclusions:

• Reduction in tangential velocity: The use of the new two-blade design resulted in a considerable decrease in the predominant tangential velocity generated by the standard two-blades. This reduction proved important in achieving better control over fluid movement in the agitated tank.

• Predominance of tangential flow: The statement emphasizes that although the tangential flow is decreased, it remains the dominant mode of fluid motion within the tank. This implies that even with a reduction in the intensity of tangential flow, it still plays a significant role in the overall fluid dynamics.

• Generation of axial flow: The new design significantly promoted the generation of axial flow in the tank, leading to a substantial increase in axial velocity. This characteristic has a positive impact in breaking sedimentation, particularly beneficial for suspensions.

• Optimized power consumption: One of the major advantages of the present study was the observation of significantly reduced power consumption. We achieved a reduction of up to 93% for certain configurations, providing a tremendous gain in energy efficiency.

• Industrial applications: The modified two-blade configurations offer practical prospects in various industrial applications, providing more efficient mixing while lowering energy costs. These improvements can benefit diverse industrial processes, such as chemical reactions, pharmaceutical production, and many others.

This innovative approach holds promising prospects for the industry in terms of energy efficiency, sustainability, and enhanced mixing performance. The obtained results have important implications for optimizing industrial processes, contributing to more sustainable and energy-efficient practices. Nevertheless, the present study serves as an initial attempt to evaluate the role of two-blades with both an enlarged and narrowed parts in order to maintain tangential predominance, activate axial mobility, and minimize energy consumption for a Newtonian fluid. Moreover, it paves the way for a more in-depth analysis of fluids with more complex rheology, such as non-Newtonian fluids and suspensions like nanofluids. Additionally, it would be beneficial to analyze mixing time by introducing a mass study, based on the concentration equation in the presence of two miscible fluids.

REFERENCES

[1] Nagata, S. (1975). Mixing: Principles and Applications. Halsted Press, New York.

[2] Xuereb, C., Poux, M., Bertrand, J. (2006). Agitation et Mélange: Aspects Fondamentaux et Applications Industrielles. Dunod, France.

[3] Ameur, H., Kamla, Y., Sahel, D. (2018). Optimization of the operating and design conditions to reduce the power consumption in a vessel stirred by a paddle impeller. Periodica Polytechnica Mechanical Engineering, 62(4): 312-319. https://doi.org/10.3311/PPme.12372

[4] Bouzit, M., Benali, L., Hachemi, M., Bouzit, F. (2006). CFD simulations of the 3D velocity profile of paddle agitator and two-blade impeller in stirred vessel with a highly viscous Newtonian fluid. Journal of Applied Sciences, 6(13): 2733-2740. https://doi.org/10.3923/jas.2006.2733.2740

[5] Laidoudi, H. (2020). Hydrodynamic analyses of the flow patterns in stirred vessel of two bladed impeller. Journal of the Serbian Society for Computational Mechanics, 14(2): 117-132. https://doi.org/10.24874/jsscm.2020.14.02.08

[6] Abld, M., Xuereb, C., Bertrand, J. (1994). Modeling of the 3D hydrodynamics of 2-blade impellers in stirred tanks filled with a highly viscous fluid. The Canadian Journal of Chemical Engineering, 72(2): 184-193. https://doi.org/10.1002/cjce.5450720202

[7] Foukrach, M., Bouzit, M., Ameur, H., Kamla, Y. (2020). Effect of agitator's types on the hydrodynamic flow in an agitated tank. Chinese Journal of Mechanical Engineering, 33(1): 1-18. https://doi.org/10.1186/s10033-020-00454-2

[8] Devi, T.T., Kumar, B. (2015). Large-eddy simulation of turbulent flow in stirred tank with a curved blade impeller. Journal of Engineering Thermophysics, 24(2): 152-168. https://doi.org/10.1134/S181023281502006X

[9] Luan, D., Zhang, S., Wei, X., Duan, Z. (2017). Effect of the 6PBT stirrer eccentricity and off-bottom clearance on mixing of pseudoplastic fluid in a stirred tank. Results in Physics, 7: 1079-1085. https://doi.org/10.1016/j.rinp.2017.02.034

[10] Youcefi, S., Bouzit, M., Ameur, H., Kamla, Y., Youcefi, A. (2013). Effect of some design parameters on the flow fields and power consumption in a vessel stirred by a Rushton turbine. Chemical and Process Engineering, 34: 293-307. https://doi.org/10.2478/cpe-2013-0024

[11] Hassouni, S., Laidoudi, H., Makinde, O.D., Bouzit, M., Haddou, B. (2023). A qualitative study of mixing a fluid inside a mechanical mixer with the effect of thermal buoyancy. Archives of Thermodynamics, 44(1): 105-119. https://doi.org/10.24425/ather.2023.145879

[12] Kamla, Y., Ameur, H., Arab, M.I., Azeddine, B. (2021). Data on the hydrodynamics and power consumption induced by modified anchor impellers in cylindrical tanks. Data in Brief, 39: 107669. https://doi.org/10.1016/j.dib.2021.107669

[13] Youcefi, S., Youcefi, A. (2015). Power consumption and mixing time in rheologically complex fluids by a two-bladed impeller. Journal of Mechanical Science and Technology, 29(2): 543–548. https://doi.org/10.1007/s12206-015-0114-1

[14] Ameur, H., Bouzit, M. (2013). Power consumption for stirring shear thinning fluids by two-blade impeller. Energy, 50: 326-332. https://doi.org/10.1016/j.energy.2012.11.016

[15] Yang, F.L., Zhou, S.J., Zhang, C.X. (2015). Turbulent flow and mixing performance of a novel six-blade grid disc impeller. Korean Journal of Chemical Engineering, 32(5): 816-825. https://doi.org/10.1007/s11814-014-0255-4

[16] Basavarajappa, M., Draper, T., Toth, P., Ring, T.A., Miskovic, S. (2015). Numerical and experimental investigation of single phase flow characteristics in stirred tanks using Rushton turbine and flotation impeller. Minerals Engineering, 83: 156-167.

https://doi.org/10.1016/j.mineng.2015.08.018

[17] Ge, C.Y., Wang, J.J., Gu, X.P., Feng, L.F. (2014). CFD simulation and PIV measurement of the flow field generated by modified pitched blade turbine impellers. Chemical Engineering Research and Design, 92(6): 1027-1036. https://doi.org/10.1016/j.cherd.2013.08.024

[18] Kato, Y., Inoue, Y., Hiramatsu, M., Ohtani, S. (2015). Mixing mechanism of large paddle impeller based on streak line observation. Kagaku Kogaku Ronbunshu, 41(1): 11-15. https://doi.org/10.1252/kakoronbunshu.41.1

[19] Kato, Y., Yasui, N., Furukawa, H., Nagumo, R. (2016). Effect of liquid height on power consumption of two-blade wide paddle impeller. Kagaku Kogaku Ronbunshu, 42(6): 187-191. https://doi.org/10.1252/kakoronbunshu.42.187

[20] Haitsuka, M., Kamei, N., Kato, Y., Kamiya, M., Furukawa, H., Nagumo, R. (2016). Power consumption and mass transfer of high viscosity liquid in gas-liquid mixing vessel with large paddle impeller. Kagaku Kogaku Ronbunshu, 42(5): 174-178. https://doi.org/10.1252/kakoronbunshu.42.174

[21] Lane, G., Koh, P.T.L. (1997). CFD simulation of a Rushton turbine in a baffled tank. In Proceedings of the International Conference on Computational Fluid Dynamics in Mineral and Metal Processing and Power Generation, CSIRO, Melbourne, pp. 377-385.

[22] Youcefi, A. (1993). Etude expérimentale de l'écoulement de fluide viscoélastique autour d'un agitateur two-blade dans une cuve agitée. Doctoral dissertation, Institut National Polytechnique, Toulouse, France.

[23] Bertrand, J. (1983). Agitation de fluides visqueux. Cas de mobiles à pales, d'ancres et de barrières. Doctoral dissertation, Institut National Polytechnique de Toulouse, France.

[24] Ameur, H. (2016). Mixing of complex fluids with flat and pitched bladed impellers: Effect of blade attack angle and shear-thinning behavior. Food and Bioproducts Processing, 99: 71-77. https://doi.org/10.1016/j.fbp.2016.04.004

[25] Ameur, H. (2017). Mixing of a viscoplastic fluid in cylindrical vessels equipped with paddle impellers. ChemistrySelect, 2(35): 11492-11496. https://doi.org/10.1002/slct.201702459

[26] Mokhefi, A., Bouanini, M., Elmir, M., Guettaf, Y., Spiteri, P (2022). Numerical investigation of mixed convection in an anchor-stirred tank filled with an Al_2O_3-water nanofluid. Chemical Papers, 1-19. https://doi.org/10.1007/s11696-021-01914-2

[27] Mokhefi, A., Bouanini, M., Elmir, M., Spitéri, P. (2021). Effect of the wavy tank wall on the characteristics of mechanical agitation in the presence of a Al_2O_3-water nanofluid. Metallurgical and Materials Engineering, 27(3): 301-320. https://doi.org/10.30544/626

[28] Montante, G., Moštěk, M., Jahoda, M., Magelli, F. (2005). CFD simulations and experimental validation of homogenisation curves and mixing time in stirred Newtonian and pseudoplastic liquids. Chemical Engineering Science, 60(8-9): 2427-2437. https://doi.org/10.1016/j.ces.2004.11.020

[29] Wang, S., Boger, D.V., Wu, J. (2012) Energy efficient solids suspension in an agitated vessel-water slurry. Chemical Engineering Science, 74: 233-243. https://doi.org/10.1016/j.ces.2012.02.035

[30] Pakzad, L., Ein-Mozaffari, F., Upreti, S. R., Lohi, A. (2013). Characterisation of the mixing of non-Newtonian fluids with a scaba 6SRGT impeller through ERT and CFD. The Canadian Journal of Chemical Engineering, 91(1): 90-100. https://doi.org/10.1002/cjce.21616

NOMENCLATURE

c	Impeller clearance [m]
D	Tank diameter [m]
d	Impeller diameter [m]
$d1$	Impeller diameter [m]
da	Shaft diameter [m]
g	Gravity [m/s^2]
H	Tank height [m]
h	Impeller height [m]
N	Impeller rotation speed [1/s]
Np	Power number [-]
p	Pressure [Pa]
P	Power [W]
Qv	Viscous dissipation function [1/s^2]
Re	Reynolds number [Pa]
t	Thickness [m]
u	x-coordinate velocity [m/s]
v	y-coordinate velocity [m/s]
V	Characteristic velocity [-]
Vo	Volume [m^3]
w	z-coordinate velocity [m]
W	Dimensionless axial velocity [-]
x	Abscissa coordinate [m]
y	Ordinate coordinate [m]
z	elevation coordinate [m]

Greek symbols

μ	Dynamic viscosity [Pa.s]
ρ	Density [kg.m^{-3}]

Index

m	Modified
r	Radial coordinate
s	Standard
θ	Tangential coordinate
$*$	Dimensionless